Edwards-Anderson parameter and local Ising nematicity in FeSe revealed via NMR spectral broadening

Paul Wiecki,[1] Rui Zhou,[2] Marc-Henri Julien,[2] Anna E. Böhmer,[1,3] and Jörg Schmalian[1,4]

[1]*Institute for Quantum Materials and Technologies, Karlsruhe Institute of Technology (KIT), 76131 Karlsruhe, Germany*

[2]*Laboratoire National des Champs Magnétiques Intenses–European Magnetic Field Laboratory, UPR3228 Centre National de la Recherche Scientifique, Université Grenoble Alpes, Institut National des Sciences Appliquées de Toulouse, Université Paul Sabatier, Grenoble, France*

[3]*Institut für Experimentalphysik IV, Ruhr-Universität Bochum, 44801 Bochum, Germany*

[4]*Institute for Theory of Condensed Matter, Karlsruhe Institute of Technology (KIT), 76131 Karlsruhe, Germany*

(Received 21 July 2021; revised 6 September 2021; accepted 8 September 2021; published 22 September 2021)

The NMR spectrum of FeSe shows a dramatic broadening on cooling towards the bulk nematic phase at $T_s = 90$ K, due to the formation of a quasistatic, short-range-ordered nematic domain structure. However, a quantitative understanding of the NMR broadening and its relationship to the nematic susceptibility is still lacking. Here, we show that the temperature and pressure dependence of the broadening is in quantitative agreement with the mean-field Edwards-Anderson parameter of an Ising-nematic model in the presence of random-field disorder introduced by nonmagnetic impurities. Furthermore, these results reconcile the interpretation of NMR and Raman spectroscopy data in FeSe under pressure.

DOI: 10.1103/PhysRevB.104.125134

I. INTRODUCTION

The nucleation of local-symmetry-breaking order in nominally symmetry-preserving phases is an increasingly recognized phenomenon in correlated electron systems. Important examples include the formation of antiferromagnetic droplets in $CeCoIn_5$, high-T_c cuprates, and low-dimensional quantum magnets [1–4], as well as the nucleation of charge density wave order above the phase transition, in $NbSe_2$ [5–7], $ZrTe_3$ [8,9], cuprates [10], and Sn/Ge(111)-α surface [11].

In the iron-based superconductors, signatures of C_4 symmetry breaking and short-range nematic order have often been found well above the bulk nematic phase transition temperature [12–15], especially from local probe measurements using scanning tunneling microscopy (STM) [16] and nuclear magnetic resonance (NMR) [17–24]. More recently, x-ray and neutron pair distribution function (PDF) studies have revealed the locally orthorhombic nature of the tetragonal paramagnetic phase in the $(Sr, Na)Fe_2As_2$ system [25]. Similarly, the re-entrant tetragonal antiferromagnetic state in this hole-doped system was also revealed to have short-range orthorhombic correlations [26]. Furthermore, inelastic x-ray scattering has recently produced insights into the spatial correlation length of nematic fluctuations in iron-based superconductors from the wave-vector-dependent softening of acoustic phonons [27–30].

While the existence of local nematicity in the tetragonal phase has been rationalized in terms of residual strains in the crystal [31], it is most naturally explained as a consequence of impurities and vacancies that locally break the fourfold rotation symmetry and thus act as random-field impurities for nematicity. Recent theoretical work has addressed the impact of disorder on the emergence of nematicity in high-temperature superconductors [32,33].

FeSe is a unique iron-based superconductor ($T_c = 8.5$ K) which has a bulk nematic phase below $T_s = 90$ K, but no corresponding magnetic phase. Several experiments have revealed a large nematic susceptibility in the high-temperature phase [34–40]. Recent NMR measurements [41–43] revealed a prominent broadening of the NMR spectrum on approaching T_s from above, which is attributed to the formation of locally nucleated, short-range-ordered nematic domains. The local orthorhombicity of unstrained FeSe above T_s was later confirmed by x-ray and neutron PDF studies [44,45] and has been used to rationalize properties of the tetragonal phase [46].

Under applied hydrostatic pressure p, the temperature-dependent full width at half maximum (FWHM) of the NMR spectrum follows a universal curve, interrupted only at the nematic transition temperature $T_s(p)$. This pressure-independent behavior of the NMR FWHM has been interpreted as evidence that the nematic fluctuations are robust against pressure application, despite the decrease of $T_s(p)$ [41,42]. However, this conclusion is in conflict with Raman spectroscopy measurements [47] which show a rapid suppression of nematic fluctuations with increasing pressure.

In order to resolve this discrepancy it is important to establish a quantitative understanding of the nematic broadening of the NMR spectrum and, in particular, its relation to the nematic susceptibility. Here, we find that the broadening of the NMR spectrum due to locally nucleated nematic order is proportional to the Edwards-Anderson parameter of a random-field Ising model at the mean-field level. Within this picture, the pressure independence of the NMR FWHM is seen to be a consequence of the pressure independence of random-field defects. We conclude that the NMR data are consistent with a suppression of nematic coupling with increasing pressure and are not in conflict with the Raman data.

II. THEORY

We consider an Ising-nematic system characterized by the pseudospin variable τ_i^z on a lattice with site i. Our analysis is independent of the microscopic origin of nematicity and equally applies to systems with spin-induced nematicity [48–51], nematicity due to orbital ordering [52–55], or systems with a Pomeranchuk instability in the $\ell = 2$ angular momentum channel [56–58]. In a clean system a finite expectation value $\phi \equiv \langle \tau^z \rangle$ corresponds to nematic order.

We allow for random strain fields $\sim h_i$ that locally break the fourfold symmetry. To be specific we consider random strain characterized by the distribution function

$$p_\sigma(h_i) = \frac{1}{\sqrt{2\pi}\sigma} e^{-\frac{h_i^2}{2\sigma^2}}. \tag{1}$$

The width σ is an energy scale that parametrizes the disorder strength. The order parameter is now $\overline{\phi} = \overline{\langle \tau^z \rangle}$, where $\langle\,\rangle$ is a thermal average and the overbar is an average over disorder configurations. Despite the random strain one still expects a sharp nematic transition above which $\overline{\phi} = 0$, at least for three-dimensional systems and not too strong disorder [59,60]. However, for the problem at hand one expects at any finite randomness a finite Edwards-Anderson parameter

$$q_{\rm EA} = \overline{\phi^2} - (\overline{\phi})^2, \tag{2}$$

that characterizes the strength of local disorder variations, even if ϕ vanishes on the average. Notice that this is different from the behavior in spin glasses where $q_{\rm EA}$ serves, at least within mean-field theory, as the "order" parameter of the spin glass state [61]. Nevertheless, there are interesting analogies between our approach and the theory of NMR in spin glasses or relaxor ferroelectrics, where the determination of the Edwards-Anderson parameter has played an important role [62–65]. In what follows we will first discuss that $q_{\rm EA}$ is directly related to the width of the NMR spectrum. In a second step we present and solve a simple mean-field model that allows for a remarkable agreement between theory and experiment.

A. Connection to NMR spectrum broadening

We start our analysis with a brief discussion of the effect of random strain on the NMR spectrum. In a homogeneous case, the NMR spectrum of a system where the nucleus under consideration has one unique position in the lattice and occurs only in one isotope configuration can be expressed as

$$f(\omega) = \frac{1}{N}\sum_{i=1}^{N} \delta(\omega - \omega_0), \tag{3}$$

where ω_0 is the Larmor frequency and N is the number of nuclei in the sample. We assume that a defect-nucleated local order parameter $\phi_i(h_i)$ will give rise to a shift of the local NMR resonance frequency according to $\omega_0 \to \omega_0 + \alpha\phi_i(h_i)$. By averaging each site over the disorder distribution $p_\sigma(h_i)$ one obtains the NMR spectrum as

$$\overline{f(\omega)} = \frac{1}{N}\int \prod_{j=1}^{N} dh_j p_\sigma(h_j) \sum_{i=1}^{N} \delta(\omega - \omega_0 - \alpha\phi_i(h_i)). \tag{4}$$

The broadening ν of the NMR spectrum is given by the second moment of the distribution $\nu^2 = \int d\omega \overline{f(\omega)}(\omega - \omega_0)^2$. Carrying through the integrations yields

$$\nu^2 = \frac{1}{N}\int \prod_{j=1}^{N} dh_j p_\sigma(h_j) \sum_{i=1}^{N} \alpha^2 \phi_i^2(h_i) \tag{5}$$

$$= \alpha^2 \overline{\phi^2} = \alpha^2 q_{\rm EA}. \tag{6}$$

Therefore, the FWHM of the NMR spectrum is expected to be proportional to the square root of the Edwards-Anderson parameter:

$$\nu = \alpha q_{\rm EA}^{1/2}. \tag{7}$$

This analysis was performed under the assumption of vanishing averaged order parameter $\overline{\phi}$. At finite $\overline{\phi}$ one easily finds that ν^2 is proportional to the expression for $q_{\rm EA}$ in Eq. (2).

B. Random-field Ising-nematic model

In order to get a quantitative understanding of the temperature and strain dependence of the Edwards-Anderson parameter $q_{\rm EA}$ of Eq. (2), we now perform a simple mean-field analysis of the corresponding random-field Ising model. While the random-field Ising model is a theoretical problem of formidable complexity, we will confine ourselves to a mean-field analysis. As we will see, this already allows for a rather detailed understanding of the temperature and pressure dependence of the NMR broadening for FeSe. Mean-field behavior of the nematic degrees of freedom is expected for clean systems. As was discussed in Ref. [66], long-range strain forces drive the statistical mechanics of the system into a mean-field regime in the entire temperature window where an appreciable softening of the shear modulus is observed. In systems with random strain, the situation is more subtle [59,60] and one expects disorder fluctuations at long distances and timescales. However, on the local length scale of the measurement of the NMR linewidth, a mean-field analysis is a reasonable starting point. The description of dynamical phenomena, as determined by the NMR relaxation rate, is likely more subtle and may require going beyond the mean-field theory.

The Hamiltonian is expressed as

$$H = -\sum_{i,j} J_{i,j}\tau_i^z\tau_j^z - \sum_i (h_0 + h_i)\tau_i^z, \tag{8}$$

where $J_{i,j}$ is the nematic coupling constant. Here, h_0 is an external strain that breaks C_4 symmetry globally, while h_i is a random field at each site. In the spirit of the mean-field analysis we approximate this model by the infinite-range interaction, where $J_{i,j} \to J/N$. Then mean-field theory becomes exact [67]. When $h_i = 0$, we obtain the familiar equation of state for the order parameter $\phi = \langle \tau^z \rangle$ is ($\beta \equiv 1/k_B T$)

$$\phi = \tanh[\beta(2J\phi + h_0)]. \tag{9}$$

The nematic transition temperature of the system without disorder follows as $T_s^{(0)} = 2J$.

If we now allow for random stress, the corresponding mean-field equation of state for the order parameter becomes

$$\overline{\phi} = \int dh p_\sigma(h) \tanh\frac{2J\overline{\phi} + h_0 + h}{k_B T}, \tag{10}$$

which is solved self-consistently for $\overline{\phi}$. To find the nematic phase transition temperature T_s/J as a function of disorder σ/J, we take $h_0 = 0$ and expand the hyperbolic tangent while keeping only terms linear in $\overline{\phi}$ to obtain

$$\overline{\phi} = \frac{2J\overline{\phi}}{k_B T_s} C\left(\frac{\sigma}{k_B T_s}\right), \tag{11}$$

where the function C is given by

$$C(t) = \int dx \frac{e^{-\frac{x^2}{2}}}{\sqrt{2\pi}} \tanh^2(xt). \tag{12}$$

The transition temperature $T_s(\sigma)$ of the system with disorder is determined by the condition

$$T_s = T_s^{(0)} C\left(\frac{\sigma}{k_B T_s}\right). \tag{13}$$

Random strain reduces the transition temperature, but the transition itself remains sharp. In distinction, global external strain h_0 would smear the transition. The nematic transition reaches $T_s = 0$ when $\sigma/J = \pi/2$. As we will see, NMR experiments for FeSe suggest that σ is significantly smaller than $\pi J/2$ where disorder destroys nematic order completely.

The nematic susceptibility above T_s is given by

$$\chi_{\rm nem}(T) = \left.\frac{\partial\overline{\phi}}{\partial h_0}\right|_{h_0=0} = \frac{C\left(\frac{\sigma}{k_B T}\right)}{T - T_s^{(0)} C\left(\frac{\sigma}{k_B T}\right)}. \tag{14}$$

As mentioned above, we have to interpret the effective Ising model as the one that includes all allowed couplings, including the ones that are mediated by the lattice. In fact, the mean-field treatment of the clean system is possible because we have included this lattice coupling which leads to an effective long-range interaction [66]. Hence, the nematic susceptibility $\chi_{\rm nem}$ is proportional to the inverse elastic constant C_{66} [50]. It diverges at the actual thermodynamic phase transition, not at the lower Curie-Weiss temperature that one deduces from Raman or elastoresistivity measurements [68].

Finally, we determine the Edwards-Anderson order parameter. Taking $h_0 = 0$ above T_s where $\overline{\phi} = 0$, we have

$$q_{\rm EA}(T) = \int dh p_\sigma(h) \tanh^2 \frac{h}{k_B T} = 1 - C\left(\frac{\sigma}{k_B T}\right). \tag{15}$$

Obviously, $q_{\rm EA}$ above T_s only depends on temperature and the strength of random strain σ. As we will see below, this explains the "scaling" of the NMR linewidth as a function of pressure. Changing the nematic coupling constant will then not change the T dependence of $q_{\rm EA}$, but will merely set the temperature $T_s = T_s^{(0)}[1 - q_{\rm EA}(T_s)]$ where it deviates from its high-temperature behavior. Clearly, the finding that $q_{\rm EA}(T > T_s)$ is independent of J is only valid within the mean-field approximation. We can turn this reasoning around and conclude that a temperature-dependent NMR linewidth that is independent of the value of T_s strongly supports that the inhomogeneous nematic state above T_s is well captured within a mean-field treatment.

We also note that the Edwards-Anderson parameter is not proportional to the nematic susceptibility. However, both are related via

$$\chi_{\rm nem}(T) = \frac{1 - q_{\rm EA}(T)}{T - T_s^{(0)}[1 - q_{\rm EA}(T)]}. \tag{16}$$

Thus, in principle it is possible to determine the Edwards-Anderson parameter from the nematic susceptibility. In practice, the available accuracy of data for $\chi_{\rm nem}(T)$ turns out not to be sufficient to determine $q_{\rm EA}(T)$. The reason is that $q_{\rm EA}(T)$ for FeSe turns out to be significantly smaller that unity. This also explains that the T dependence of $q_{\rm EA}$ does not significantly change the Curie-Weiss behavior of the nematic susceptibility. Thus $\chi_{\rm nem}$ is not a sensitive indicator of inhomogeneous nematicity while local probes, such as NMR linewidth measurements, are able to reveal the existence and temperature dependence of inhomogeneous nematic regions.

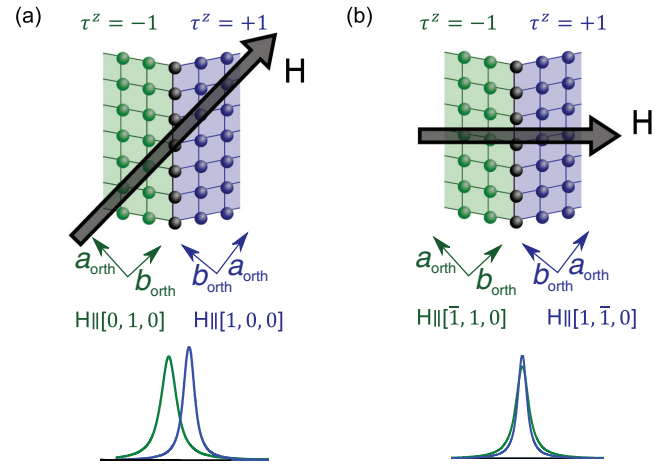

FIG. 1. The Ising variable $\tau^z = \pm 1$ breaks the fourfold symmetry in two different ways, resulting in the formation of domains when local nematic order is present. In (a), a magnetic field H is applied such that the nuclei in the two domains experience symmetry-inequivalent field directions. Due to the anisotropy of magnetic susceptibility in the nematic state, the nuclei in the two domains see different local hyperfine fields, resulting in a two-peak NMR spectrum, as illustrated schematically. In contrast, when the field is rotated 45° as in (b), the nuclei experience symmetry equivalent hyperfine fields, and the NMR spectrum appears as a single peak.

III. SUMMARY OF NMR RESULTS

Since ^{77}Se is an $I = 1/2$ nucleus, there are no quadrupole satellite lines or quadrupole shifts of the spectrum. Therefore, in the high-temperature tetragonal state, the NMR spectrum is a single peak. In the nematic state below T_s, there are nematic-twin domains. As illustrated in Fig. 1(a), half of the domains experience $H \| a_O$ ($H \| [100]_O$) and the other half experience $H \| b_O$ ($H \| [010]_O$), where $a_O > b_O$. Due to the anisotropic magnetic susceptibility of the nematic phase [70,71], the hyperfine field at the nucleus will be different in the two domains, causing the NMR spectrum to split into two peaks in the nematic ordered state. If the field is instead applied along $H \| [110]_O$ [Fig. 1(b)], then both types of domain see a symmetry-equivalent magnetic field, and there is only a single NMR peak in the nematic state, even though there are still domains. Recent NMR measurements under mechanical

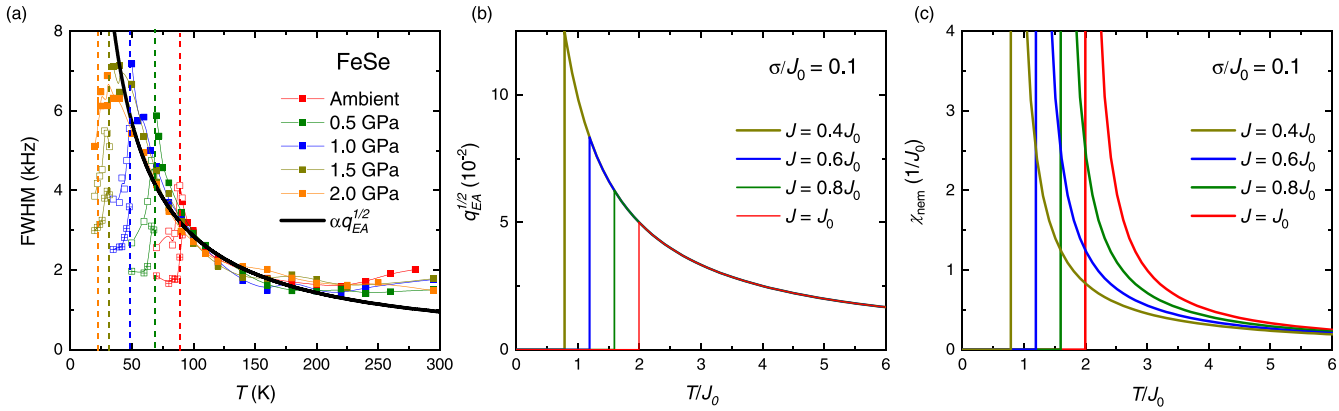

FIG. 2. (a) FWHM of ^{77}Se NMR spectrum in FeSe under indicated hydrostatic pressures [41]. Overlaid is the scaled Edwards-Anderson parameter $\alpha q_{\rm EA}^{1/2}$ for disorder strength $\sigma/J = 0.1$ and $T_s = 30$ K. Vertical dashed lines denote T_s. Note that at 2.0 GPa, T_s becomes a joint nematic-magnetic transition [69]. Below T_s, the FWHM of the low-frequency NMR peak (open symbols) is greater than that of the high-frequency peak (hatched symbols). (b) Square root of the Edwards-Anderson parameter $q_{\rm EA}^{1/2}$ for decreasing values of nematic coupling J at constant disorder strength σ. J_0 corresponds to the strength of the nematic coupling at ambient pressure, while pressure reduces J below J_0. Notice that $q_{\rm EA}$ above T_s is independent of this nematic interaction J. (c) Nematic susceptibility $\chi_{\rm nem}$ for decreasing values of nematic coupling J at constant disorder strength σ. The pressure-independent behavior of the NMR FWHM in the paramagnetic state (a) resembles the Edwards-Anderson parameter $q_{\rm EA}^{1/2}$ (b) and not the nematic susceptibility $\chi_{\rm nem}$ (c), as anticipated theoretically in Eq. (7).

strain have revealed that the higher-frequency NMR peak comes from the domains which experience $H\|a_O$, while the lower-frequency peak comes from the $H\|b_O$ domains [71].

In the tetragonal phase, the FWHM of the single NMR peak increases on cooling towards the nematic state. However, this broadening is observed only when $H\|[100]_O$ and not when $H\|[110]_O$ [41,42]. This observation provides clear evidence that the broadening is related to nematicity and implies the existence of a short-range nematic domain structure in the tetragonal state of FeSe. Since this effect is observed in the NMR spectrum, the fluctuating nematic domain structure is static on the timescale set by the inverse NMR linewidth $\sim 1/(1\ \text{kHz})$.

IV. COMPARISON OF THEORY AND EXPERIMENT

For a direct comparison between theory and experiment FeSe offers several clear advantages over other nematic iron-based superconductors. First, FeSe has no bulk magnetic phase at ambient pressure, and thus the pure Ising-nematic model is expected to be relevant in this system. Second, the ^{77}Se nucleus has $I = 1/2$ so that no complications arise from nuclear quadrupole couplings. Finally, no dopants are present, which can introduce additional lines into the NMR spectrum [17,72].

Figure 2(a) shows the NMR FWHM data for FeSe under pressure. The FWHM increases on cooling towards T_s. The data at different pressures follow a universal curve, simply interrupted at the appropriate nematic transition temperatures $T_s(p)$. Below $T_s(p)$ in the nematic state, the FWHM of each of the two NMR peaks is shown separately. The FWHM of the low-frequency NMR peak (open symbols) is greater than that of the high-frequency peak (hatched symbols). The different FWHM of the two NMR peaks in the nematic state of FeSe has been noted in independent measurements and is currently not understood [71].

Within the Ising-nematic model, the experimental data under pressure are expected to correspond to a constant disorder strength σ (determined only by the disorder of the particular crystal), but decreasing nematic coupling J, starting from a value J_0 that corresponds to ambient pressure. Figures 2(b) and 2(c) show the mean-field behavior of the Edwards-Anderson parameter $q_{\rm EA}^{1/2}$ and the nematic susceptibility $\chi_{\rm nem}$ under these assumptions. As expected, the NMR data are well described by $q_{\rm EA}^{1/2}$ and not $\chi_{\rm nem}$ [Eq. (7)]. The universal FWHM curve followed at all pressures is seen to be the result of the constant σ. The existence of a universal curve does not mean that the nematic tendency is somehow independent of pressure, as proposed in both NMR papers [41,42]. Rather, this reflects the fact that $q_{\rm EA}(T > T_s)$ is independent of J within the mean-field approximation, as discussed above. Therefore, the NMR data are consistent with the Raman data, showing a suppression of nematic fluctuations [Fig. 2(c)] under pressure [47].

The FWHM data in Fig. 2(a) show a deviation from $q_{\rm EA}^{1/2}$ at high temperature. This deviation is easily understood. In a usual paramagnetic state, the broadening reflects the spatial distribution of K values due to sample inhomogeneity, and the temperature dependence of the broadening typically follows the temperature dependence of the magnetic susceptibility $\chi_{\rm mag}$. In FeSe, both $\chi_{\rm mag}$ [38] and the NMR shift [35,41,73] increase with warming, and therefore the NMR spectrum is expected to broaden on warming. At high temperatures ($T \gtrsim 200$ K), the nematic broadening described by $q_{\rm EA}$ is small and the NMR FWHM is dominated by standard inhomogeneous broadening that increases with increasing temperature. At lower temperatures, the short-range nematic domain structure becomes the dominant source of broadening and the FWHM increases upon decreasing temperature [41].

At 2 GPa, the FWHM data appear to level off just above the T_s. At this pressure, the T_s is a joint structural-magnetic transition [69]. Here, the simple Ising-nematic model may no

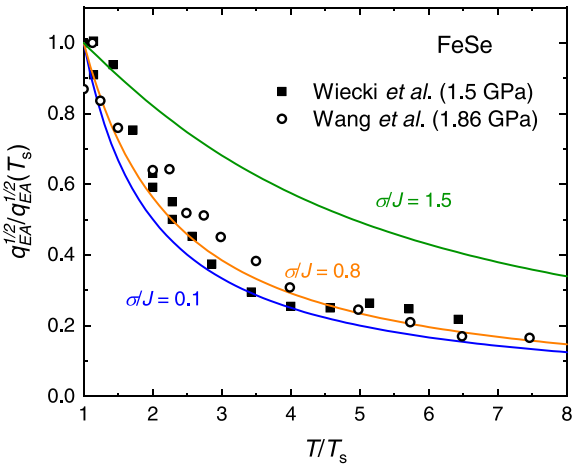

FIG. 3. NMR FWHM in FeSe normalized at T_s as a function of T/T_s at indicated hydrostatic pressures [41,42]. The data are compared to $q_{\mathrm{EA}}^{1/2}/q_{\mathrm{EA}}^{1/2}(T_s)$ calculated in the random-field Ising-nematic model at the mean-field level. The only adjustable parameter is the disorder strength σ/J. For $\sigma/J > \pi/2$, there is no long-range nematic order.

longer be applicable when the ground state is no longer pure nematic.

A more detailed comparison of theory and experiment is shown in Fig. 3, where we plot the FWHM (normalized at T_s) as a function of reduced temperature T/T_s for both NMR studies [41,42]. We note that the FWHM at T_s differs in the two studies due to different amounts of disorder in the two crystals. Here, we plot the data at high pressure so that T_s is reduced and the data can be compared with the Ising-nematic model over the largest temperature range. The only adjustable parameter in the model is the disorder strength σ/J. Here, the NMR data are compared with $\sigma/J = 0.1$, 0.8, and 1.5. For $\sigma/J > \pi/2$, there is no long-range nematic order due to the strong disorder. The NMR data agree well with the theoretical curves at small disorder parameters, as expected.

V. CONCLUSIONS

FeSe features a local, orthorhombic nematic order in its high-temperature, nominally tetragonal phase. The observed agreement between the NMR line broadening and the Edwards-Anderson parameter of the disordered, random-field Ising-nematic model implies that this local nematic order is primarily nucleated by crystal defects. The origin of the local orthorhombicity was not explicitly considered in the PDF studies of FeSe [44,45]. We note that this short-range-ordered nematicity in the high-temperature tetragonal state is distinct from the quantum Griffiths phase recently proposed in Fe(Se,S) under pressure, where rare but large regions of local nematic droplets undergo quantum fluctuations [74]. In this context it is important to keep in mind that in metallic systems such quantum fluctuations are known to be strongly suppressed due to the coupling to the particle-hole continuum [75–77], a behavior specific to Ising degrees of freedom [78]. In fact, it is this suppression of quantum fluctuations that is consistent with the effectively classical description of local nematic order of our approach. Finally, our results demonstrate that the nematic fluctuations in FeSe are suppressed by hydrostatic pressure, consistent with Raman studies [47], despite the pressure independence of the nematic broadening of the NMR lines. This understanding could be further confirmed by elastoresistance measurements inside a pressure cell [79].

ACKNOWLEDGMENTS

We thank B. M. Andersen, S. A. Kivelson, R. M. Fernandes, and Y. Furukawa for valuable discussions. We acknowledge support by the Helmholtz Association under Contract No. VH-NG-1242. This work was also supported by the German Research Foundation (DFG) under CRC/TRR 288 – 422213477 Elasto-Q-Mat (Projects A02 and B01). Work in Grenoble was supported by the Laboratoire d'Excellence LANEF (ANR-10-LABX-51-01) and by the French Agence Nationale de la Recherche (ANR) under Reference No. ANR-19-CE30-0019 (Neptun).

[1] R. R. Urbano, B.-L. Young, N. J. Curro, J. D. Thompson, L. D. Pham, and Z. Fisk, Interacting Antiferromagnetic Droplets in Quantum Critical $CeCoIn_5$, Phys. Rev. Lett. **99**, 146402 (2007).

[2] S. Seo, X. Lu, J.-X. Zhu, R. R. Urbano, N. Curro, E. D. Bauer, V. A. Sidorov, L. D. Pham, T. Park, Z. Fisk, and J. D. Thompson, Disorder in quantum critical superconductors, Nat. Phys. **10**, 120 (2013).

[3] M.-H. Julien, T. Fehér, M. Horvatić, C. Berthier, O. N. Bakharev, P. Ségransan, G. Collin, and J.-F. Marucco, ^{63}Cu NMR Evidence for Enhanced Antiferromagnetic Correlations Around Zn Impurities in $YBa_2Cu_3O_{6.7}$, Phys. Rev. Lett. **84**, 3422 (2000).

[4] H. Kimura, M. Kofu, Y. Matsumoto, and K. Hirota, Novel In-Gap Spin State in Zn-Doped $La_{1.85}Sr_{0.15}CuO_4$, Phys. Rev. Lett. **91**, 067002 (2003).

[5] C. Berthier, D. Jerome, and C. Molinie, NMR study on a 2H-$NbSe_2$ single crystal: A microscopic investigation of the charge density waves state, J. Phys. C: Solid State Phys. **11**, 797 (1978).

[6] C. J. Arguello, S. P. Chockalingam, E. P. Rosenthal, L. Zhao, C. Gutiérrez, J. H. Kang, W. C. Chung, R. M. Fernandes, S. Jia, A. J. Millis, R. J. Cava, and A. N. Pasupathy, Visualizing the charge density wave transition in 2H-$NbSe_2$ in real space, Phys. Rev. B **89**, 235115 (2014).

[7] U. Chatterjee, J. Zhao, M. Iavarone, R. Di Capua, J. P. Castellan, G. Karapetrov, C. D. Malliakas, M. G. Kanatzidis, H. Claus, J. P. C. Ruff, F. Weber, J. van Wezel, J. C. Campuzano, R. Osborn, M. Randeria, N. Trivedi, M. R. Norman, and S. Rosenkranz, Emergence of coherence in the charge-density wave state of 2H-$NbSe_2$, Nat. Commun. **6**, 6313 (2015).

[8] L. Yue, S. Xue, J. Li, W. Hu, A. Barbour, F. Zheng, L. Wang, J. Feng, S. B. Wilkins, C. Mazzoli, R. Comin, and Y. Li, Distinction between pristine and disorder-perturbed charge density waves in $ZrTe_3$, Nat. Commun. **11**, 98 (2020).

[9] L. Liu, C. Zhu, Z. Y. Liu, H. Deng, X. B. Zhou, Y. Li, Y. Sun, X. Huang, S. Li, X. Du, Z. Wang, T. Guan, H. Mao, Y. Sui, R. Wu, J.-X. Yin, J. G. Cheng, and S. H. Pan, Thermal Dynamics of Charge Density Wave Pinning in $ZrTe_3$, Phys. Rev. Lett. **126**, 256401 (2021).

[10] T. Wu, H. Mayaffre, S. Krämer, M. Horvatić, C. Berthier, W. N. Hardy, R. Liang, D. A. Bonn, and M.-H. Julien, Incipient charge order observed by NMR in the normal state of $YBa_2Cu_3O_y$, Nat. Commun. **6**, 6438 (2015).

[11] H. H. Weitering, J. M. Carpinelli, A. V. Melechko, J. Zhang, M. Bartkowiak, and E. W. Plummer, Defect-mediated condensation of a charge density wave, Science **285**, 2107 (1999).

[12] S. Kasahara, H. J. Shi, K. Hashimoto, S. Tonegawa, Y. Mizukami, T. Shibauchi, K. Sugimoto, T. Fukuda, T. Terashima, A. H. Nevidomskyy, and Y. Matsuda, Electronic nematicity above the structural and superconducting transition in $BaFe_2(As_{1-x}P_x)_2$, Nature (London) **486**, 382 (2012).

[13] M. Yi, D. Lu, J.-H. Chu, J. G. Analytis, A. P. Sorini, A. F. Kemper, B. Moritz, S.-K. Mo, R. G. Moore, M. Hashimoto, W.-S. Lee, Z. Hussain, T. P. Devereaux, I. R. Fisher, and Z.-X. Shen, Symmetry-breaking orbital anisotropy observed for detwinned $Ba(Fe_{1-x}Co_x)_2As_2$ above the spin density wave transition, Proc. Natl. Acad. Sci. USA **108**, 6878 (2011).

[14] W. Wang, Y. Song, C. Cao, K.-F. Tseng, T. Keller, Y. Li, L. W. Harriger, W. Tian, S. Chi, R. Yu, A. H. Nevidomskyy, and P. Dai, Local orthorhombic lattice distortions in the paramagnetic tetragonal phase of superconducting $NaFe_{1-x}Ni_xAs$, Nat. Commun. **9**, 3128 (2018).

[15] X. Hong, F. Caglieris, R. Kappenberger, S. Wurmehl, S. Aswartham, F. Scaravaggi, P. Lepucki, A. U. B. Wolter, H.-J. Grafe, B. Büchner, and C. Hess, Evolution of the Nematic Susceptibility in $LaFe_{1-x}Co_xAsO$, Phys. Rev. Lett. **125**, 067001 (2020).

[16] E. P. Rosenthal, E. F. Andrade, C. J. Arguello, R. M. Fernandes, L. Y. Xing, X. C. Wang, C. Q. Jin, A. J. Millis, and A. N. Pasupathy, Visualization of electron nematicity and unidirectional antiferroic fluctuations at high temperatures in NaFeAs, Nat. Phys. **10**, 225 (2014).

[17] T. Iye, M.-H. Julien, H. Mayaffre, M. Horvatić, C. Berthier, K. Ishida, H. Ikeda, S. Kasahara, T. Shibauchi, and Y. Matsuda, Emergence of orbital nematicity in the tetragonal phase of $BaFe_2(As_{1-x}P_x)_2$, J. Phys. Soc. Jpn. **84**, 043705 (2015).

[18] R. Zhou, L. Y. Xing, X. C. Wang, C. Q. Jin, and G.-q. Zheng, Orbital order and spin nematicity in the tetragonal phase of the electron-doped iron pnictides $NaFe_{1-x}Co_xAs$, Phys. Rev. B **93**, 060502(R) (2016).

[19] M. Toyoda, Y. Kobayashi, and M. Itoh, Nematic fluctuations in iron arsenides NaFeAs and LiFeAs probed by ^{75}As NMR, Phys. Rev. B **97**, 094515 (2018).

[20] M. Toyoda, A. Ichikawa, Y. Kobayashi, M. Sato, and M. Itoh, In-plane anisotropy of the electric field gradient in $Ba(Fe_{1-x}Co_x)_2As_2$ observed by ^{75}As NMR, Phys. Rev. B **97**, 174507 (2018).

[21] A. P. Dioguardi, M. M. Lawson, B. T. Bush, J. Crocker, K. R. Shirer, D. M. Nisson, T. Kissikov, S. Ran, S. L. Bud'ko, P. C. Canfield, S. Yuan, P. L. Kuhns, A. P. Reyes, H.-J. Grafe, and N. J. Curro, NMR evidence for inhomogeneous glassy behavior driven by nematic fluctuations in iron arsenide superconductors, Phys. Rev. B **92**, 165116 (2015).

[22] A. P. Dioguardi, T. Kissikov, C. H. Lin, K. R. Shirer, M. M. Lawson, H.-J. Grafe, J.-H. Chu, I. R. Fisher, R. M. Fernandes, and N. J. Curro, NMR Evidence for Inhomogeneous Nematic Fluctuations in $BaFe_2(As_{1-x}P_x)_2$, Phys. Rev. Lett. **116**, 107202 (2016).

[23] L. Bossoni, P. Carretta, W. P. Halperin, S. Oh, A. Reyes, P. Kuhns, and P. C. Canfield, Evidence of unconventional low-frequency dynamics in the normal phase of $Ba(Fe_{1-x}Rh_x)_2As_2$ iron-based superconductors, Phys. Rev. B **88**, 100503(R) (2013).

[24] L. Bossoni, M. Moroni, M. H. Julien, H. Mayaffre, P. C. Canfield, A. Reyes, W. P. Halperin, and P. Carretta, Persistence of slow fluctuations in the overdoped regime of $Ba(Fe_{1-x}Rh_x)_2As_2$ superconductors, Phys. Rev. B **93**, 224517 (2016).

[25] B. A. Frandsen, K. M. Taddei, D. E. Bugaris, R. Stadel, M. Yi, A. Acharya, R. Osborn, S. Rosenkranz, O. Chmaissem, and R. J. Birgeneau, Widespread orthorhombic fluctuations in the $(Sr, Na)Fe_2As_2$ family of superconductors, Phys. Rev. B **98**, 180505(R) (2018).

[26] B. A. Frandsen, K. M. Taddei, M. Yi, A. Frano, Z. Guguchia, R. Yu, Q. Si, D. E. Bugaris, R. Stadel, R. Osborn, S. Rosenkranz, O. Chmaissem, and R. J. Birgeneau, Local Orthorhombicity in the Magnetic C_4 Phase of the Hole-Doped Iron-Arsenide Superconductor $Sr_{1-x}Na_xFe_2As_2$, Phys. Rev. Lett. **119**, 187001 (2017).

[27] S. Wu, Y. Song, Y. He, A. Frano, M. Yi, X. Chen, H. Uchiyama, A. Alatas, A. H. Said, L. Wang, T. Wolf, C. Meingast, and R. J. Birgeneau, Short-Range Nematic Fluctuations in $Sr_{1-x}Na_xFe_2As_2$ Superconductors, Phys. Rev. Lett. **126**, 107001 (2021).

[28] F. Weber, D. Parshall, L. Pintschovius, J.-P. Castellan, M. Kauth, M. Merz, Th. Wolf, M. Schütt, J. Schmalian, R. M. Fernandes, and D. Reznik, Soft phonons reveal the nematic correlation length in $Ba(Fe_{0.94}Co_{0.06})_2As_2$, Phys. Rev. B **98**, 014516 (2018).

[29] A. M. Merritt, F. Weber, J.-P. Castellan, Th. Wolf, D. Ishikawa, A. H. Said, A. Alatas, R. M. Fernandes, A. Q. R. Baron, and D. Reznik, Nematic Correlation Length in Iron-Based Superconductors Probed by Inelastic X-Ray Scattering, Phys. Rev. Lett. **124**, 157001 (2020).

[30] M. Kauth, S. Rosenkranz, A. H. Said, K. M. Taddei, Th. Wolf, and F. Weber, Soft elastic constants from phonon spectroscopy in hole-doped $Ba_{1-x}(K, Na)_xFe_2As_2$ and $Sr_{1-x}Na_xFe_2As_2$, Phys. Rev. B **102**, 144526 (2020).

[31] S.-H. Baek, D. V. Efremov, J. M. Ok, J. S. Kim, J. van den Brink, and B. Büchner, Nematicity and in-plane anisotropy of superconductivity in β-FeSe detected by ^{77}Se nuclear magnetic resonance, Phys. Rev. B **93**, 180502(R) (2016).

[32] L. Nie, G. Tarjus, and S. A. Kivelson, Quenched disorder and vestigial nematicity in the pseudogap regime of the cuprates, Proc. Natl. Acad. Sci. USA **111**, 7980 (2014).

[33] D. Steffensen, P. Kotetes, I. Paul, and B. M. Andersen, Disorder-induced electronic nematicity, Phys. Rev. B **100**, 064521 (2019).

[34] M. D. Watson, T. K. Kim, A. A. Haghighirad, N. R. Davies, A. McCollam, A. Narayanan, S. F. Blake, Y. L. Chen, S. Ghannadzadeh, A. J. Schofield, M. Hoesch, C. Meingast, T. Wolf, and A. I. Coldea, Emergence of the nematic electronic state in FeSe, Phys. Rev. B **91**, 155106 (2015).

[35] A. E. Böhmer, T. Arai, F. Hardy, T. Hattori, T. Iye, T. Wolf, H. v. Löhneysen, K. Ishida, and C. Meingast, Origin of the Tetragonal-to-Orthorhombic Phase Transition in FeSe: A Combined Thermodynamic and NMR Study of Nematicity, Phys. Rev. Lett. **114**, 027001 (2015).

[36] C.-W. Luo, P. C. Cheng, S.-H. Wang, J.-C. Chiang, J.-Y. Lin, K.-H. Wu, J.-Y. Juang, D. A. Chareev, O. S. Volkova, and A. N. Vasiliev, Unveiling the hidden nematicity and spin subsystem in FeSe, npj Quantum Mater. **2**, 32 (2017).

[37] P. Massat, D. Farina, I. Paul, S. Karlsson, P. Strobel, P. Toulemonde, M.-A. Méasson, M. Cazayous, A. Sacuto, S. Kasahara, T. Shibauchi, Y. Matsuda, and Y. Gallais, Charge-induced nematicity in FeSe, Proc. Natl. Acad. Sci. USA **113**, 9177 (2016).

[38] A. E. Böhmer and A. Kreisel, Nematicity, magnetism and superconductivity in FeSe, J. Phys.: Condens. Matter **30**, 023001 (2017).

[39] S. Hosoi, K. Matsuura, K. Ishida, H. Wang, Y. Mizukami, T. Watashige, S. Kasahara, Y. Matsuda, and T. Shibauchi, Nematic quantum critical point without magnetism in $FeSe_{1-x}S_x$ superconductors, Proc. Natl. Acad. Sci. USA **113**, 8139 (2016).

[40] J. M. Bartlett, A. Steppke, S. Hosoi, H. Noad, J. Park, C. Timm, T. Shibauchi, A. P. Mackenzie, and C. W. Hicks, Relationship between Transport Anisotropy and Nematicity in FeSe, Phys. Rev. X **11**, 021038 (2021).

[41] P. Wiecki, M. Nandi, A. E. Böhmer, S. L. Bud'ko, P. C. Canfield, and Y. Furukawa, NMR evidence for static local nematicity and its cooperative interplay with low-energy magnetic fluctuations in FeSe under pressure, Phys. Rev. B **96**, 180502(R) (2017).

[42] P. S. Wang, P. Zhou, S. S. Sun, Y. Cui, T. R. Li, H. Lei, Z. Wang, and W. Yu, Robust short-range-ordered nematicity in FeSe evidenced by high-pressure NMR, Phys. Rev. B **96**, 094528 (2017).

[43] J. Li, B. Lei, D. Zhao, L. P. Nie, D. W. Song, L. X. Zheng, S. J. Li, B. L. Kang, X. G. Luo, T. Wu, and X. H. Chen, Spin-Orbital-Intertwined Nematic State in FeSe, Phys. Rev. X **10**, 011034 (2020).

[44] R. J. Koch, T. Konstantinova, M. Abeykoon, A. Wang, C. Petrovic, Y. Zhu, E. S. Bozin, and S. J. L. Billinge, Room temperature local nematicity in FeSe superconductor, Phys. Rev. B **100**, 020501(R) (2019).

[45] B. A. Frandsen, Q. Wang, S. Wu, J. Zhao, and R. J. Birgeneau, Quantitative characterization of short-range orthorhombic fluctuations in FeSe through pair distribution function analysis, Phys. Rev. B **100**, 020504(R) (2019).

[46] Z. Wang, X.-G. Zhao, R. Koch, S. J. L. Billinge, and A. Zunger, Understanding electronic peculiarities in tetragonal FeSe as local structural symmetry breaking, Phys. Rev. B **102**, 235121 (2020).

[47] P. Massat, Y. Quan, R. Grasset, M.-A. Méasson, M. Cazayous, A. Sacuto, S. Karlsson, P. Strobel, P. Toulemonde, Z. Yin, and Y. Gallais, Collapse of Critical Nematic Fluctuations in FeSe under Pressure, Phys. Rev. Lett. **121**, 077001 (2018).

[48] C. Xu, M. Müller, and S. Sachdev, Ising and spin orders in the iron-based superconductors, Phys. Rev. B **78**, 020501(R) (2008).

[49] C. Fang, H. Yao, W.-F. Tsai, J. Hu, and S. A. Kivelson, Theory of electron nematic order in LaFeAsO, Phys. Rev. B **77**, 224509 (2008).

[50] R. M. Fernandes, L. H. VanBebber, S. Bhattacharya, P. Chandra, V. Keppens, D. Mandrus, M. A. McGuire, B. C. Sales, A. S. Sefat, and J. Schmalian, Effects of Nematic Fluctuations on the Elastic Properties of Iron Arsenide Superconductors, Phys. Rev. Lett. **105**, 157003 (2010).

[51] R. M. Fernandes, A. V. Chubukov, and J. Schmalian, What drives nematic order in iron-based superconductors?, Nat. Phys. **10**, 97 (2014).

[52] F. Krüger, S. Kumar, J. Zaanen, and J. van den Brink, Spin-orbital frustrations and anomalous metallic state in iron-pnictide superconductors, Phys. Rev. B **79**, 054504 (2009).

[53] W. Lv, J. Wu, and P. Phillips, Orbital ordering induces structural phase transition and the resistivity anomaly in iron pnictides, Phys. Rev. B **80**, 224506 (2009).

[54] C.-C. Chen, J. Maciejko, A. P. Sorini, B. Moritz, R. R. P. Singh, and T. P. Devereaux, Orbital order and spontaneous orthorhombicity in iron pnictides, Phys. Rev. B **82**, 100504(R) (2010).

[55] H. Kontani and S. Onari, Orbital-Fluctuation-Mediated Superconductivity in Iron Pnictides: Analysis of the Five-Orbital Hubbard-Holstein Model, Phys. Rev. Lett. **104**, 157001 (2010).

[56] V. Oganesyan, S. A. Kivelson, and E. Fradkin, Quantum theory of a nematic Fermi fluid, Phys. Rev. B **64**, 195109 (2001).

[57] H. Yamase, V. Oganesyan, and W. Metzner, Mean-field theory for symmetry-breaking Fermi surface deformations on a square lattice, Phys. Rev. B **72**, 035114 (2005).

[58] A. V. Chubukov, M. Khodas, and R. M. Fernandes, Magnetism, Superconductivity, and Spontaneous Orbital Order in Iron-Based Superconductors: Which Comes First and Why? Phys. Rev. X **6**, 041045 (2016).

[59] T. Nattermann, Dipolar interaction in random-field systems, J. Phys. A: Math. Gen. **21**, L645 (1988).

[60] H. S. Toh, Structural phase transitions with random strains, J. Phys. A: Math. Gen. **25**, 4767 (1992).

[61] K. H. Fischer and J. A. Hertz, *Spin Glasses*, Cambridge Studies in Magnetism (Cambridge University Press, Cambridge, UK, 1991).

[62] R. Blinc, NQR in dipolar and quadrupolar glasses, Z. Naturforsch. A **45**, 313 (1990).

[63] S. Chen and D. C. Ailion, NMR determination of the Edwards-Anderson order parameter in the deuterated pseudo-spin-glass $Rb_{1-x}(ND_4)_xD_2PO_4$: Anisotropy and concentration dependence of the ND_4^+ deuteron second moment, Phys. Rev. B **42**, 5945 (1990).

[64] G. Papantopoulos, G. Papavassiliou, F. Milia, V. H. Schmidt, J. E. Drumheller, N. J. Pinto, R. Blinc, and B. Zalar, ^{75}As Nuclear Quadrupole Resonance in Weakly Substitutionally Disordered $Rb_{1-x}(NH_4)_xH_2AsO_4$, Phys. Rev. Lett. **73**, 276 (1994).

[65] R. Blinc, J. Dolinšek, A. Gregorovič, B. Zalar, C. Filipič, Z. Kutnjak, A. Levstik, and R. Pirc, Local Polarization Distribution and Edwards-Anderson Order Parameter of Relaxor Ferroelectrics, Phys. Rev. Lett. **83**, 424 (1999).

[66] U. Karahasanovic and J. Schmalian, Elastic coupling and spin-driven nematicity in iron-based superconductors, Phys. Rev. B **93**, 064520 (2016).

[67] T. Schneider and E. Pytte, Random-field instability of the ferromagnetic state, Phys. Rev. B **15**, 1519 (1977).

[68] Y. Gallais and I. Paul, Charge nematicity and electronic Raman scattering in iron-based superconductors, C. R. Phys. **17**, 113 (2016).

[69] K. Kothapalli, A. E. Böhmer, W. T. Jayasekara, B. G. Ueland, P. Das, A. Sapkota, V. Taufour, Y. Xiao, E. Alp, S. L. Bud'ko, P. C. Canfield, A. Kreyssig, and A. I. Goldman, Strong cooperative coupling of pressure-induced magnetic order and nematicity in FeSe, Nat. Commun. **7**, 12728 (2016).

[70] M. He, L. Wang, F. Hardy, L. Xu, T. Wolf, P. Adelmann, and C. Meingast, Evidence for short-range magnetic order in the nematic phase of FeSe from anisotropic in-plane magnetostriction and susceptibility measurements, Phys. Rev. B **97**, 104107 (2018).

[71] R. Zhou, D. D. Scherer, H. Mayaffre, P. Toulemonde, M. Ma, Y. Li, B. M. Andersen, and M.-H. Julien, Singular magnetic anisotropy in the nematic phase of FeSe, npj Quantum Mater. **5**, 93 (2020).

[72] F. L. Ning, K. Ahilan, T. Imai, A. S. Sefat, M. A. McGuire, B. C. Sales, D. Mandrus, P. Cheng, B. Shen, and H.-H. Wen, Contrasting Spin Dynamics between Underdoped and Overdoped $Ba(Fe_{1-x}Co_x)_2As_2$, Phys. Rev. Lett. **104**, 037001 (2010).

[73] S.-H. Baek, D. V. Efremov, J. M. Ok, J. S. Kim, J. van den Brink, and B. Büchner, Orbital-driven nematicity in FeSe, Nat. Mater. **14**, 210 (2014).

[74] P. Reiss, D. Graf, A. A. Haghighirad, T. Vojta, and A. I. Coldea, Signatures of a quantum Griffiths phase close to an electronic nematic quantum phase transition, arXiv:2103.07991.

[75] A. J. Millis, D. K. Morr, and J. Schmalian, Local Defect in Metallic Quantum Critical Systems, Phys. Rev. Lett. **87**, 167202 (2001).

[76] A. J. Millis, D. K. Morr, and J. Schmalian, Quantum Griffiths effects in metallic systems, Phys. Rev. B **66**, 174433 (2002).

[77] T. Vojta, Disorder-Induced Rounding of Certain Quantum Phase Transitions, Phys. Rev. Lett. **90**, 107202 (2003).

[78] T. Vojta and J. Schmalian, Quantum Griffiths effects in itinerant Heisenberg magnets, Phys. Rev. B **72**, 045438 (2005).

[79] E. Gati, L. Xiang, S. L. Bud'ko, and P. C. Canfield, Measurements of elastoresistance under pressure by combining in-situ tunable quasi-uniaxial stress with hydrostatic pressure, Rev. Sci. Instrum. **91**, 023904 (2020).